Thermal Conductivity of Iron–Titanium Powders

Te-Hua Lin,† Jack S. Watson,* and Paul W. Fisher

Chemical Technology Division, Oak Ridge National Laboratory, Oak Ridge, Tennessee 37831

Effective thermal conductivities for beds of deactivated, granular iron–titanium alloy have been measured over a range of hydrogen pressures from 0.1 to 35 atm (0.01–3.5 MPa) and over a temperature range from 10 to 75 °C (283–348 K). At approximately 40 °C (313 K), the conductivity rises almost linearly from 1.18 Btu/(h·ft·°F), or 2.04 W/(m·K), at 1 atm to 1.27 Btu/(h·ft·°F), or 2.20 W/(m·K), at 35 atm (3.5 MPa). The conductivity varies inversely with temperature over the range studied. Good agreement was obtained between values calculated from heating and cooling curves, indicating that a hydriding reaction did not occur. Conductivities were also measured with helium, nitrogen, and argon cover gas. The thermal conductivity of an iron–titanium granular bed containing reticulated aluminum foam was found to be a factor of ~1.4 higher than that for the iron–titanium alone.

Introduction

Fe–Ti is one of several hydride-forming alloys that have been considered for dense, low-pressure storage of hydrogen (often for use as a fuel) and/or for use in chemical heat pumps that utilize exothermic/endothermic hydriding/dehydriding reactions (*1–4*). Efficient and rapid removal of the heat of reaction is necessary in each of these applications. As a fuel storage medium, good heat transfer is needed to provide rapid fuel loading and to allow acceptable fuel discharge rates using only low-grade heat from combustion (or fuel-cell) exhaust gases. In heat pump applications the heat-exchange rate determines the productivity of the system, and all excess temperature differences (driving forces) required to achieve acceptable rates contribute to thermal inefficiencies of the system.

In a bed of alloy powder, heat is transferred from the reaction zone to the heated or cooled surface through the powder; and since the effective thermal conductivity of this medium is low, heat transfer usually controls the bed performance (*5–7*). Most techniques for improving heat transfer within hydride beds involve adding heat-transfer surfaces within the bed to reduce the distance over which heat must travel through the low-conductivity powder. One suggested approach (*8*) would use reticulated aluminum foam within the bed. Analysis and engineering design of these beds require reliable data on their thermal conductivities for use in mathematical models that describe the heat-transfer processes occurring during hydrogen loading and discharge. After the initial hydride cycle, the individual powder particles become highly fractured, and the resulting irregular shapes and porosity of individual particles make estimation of conductivities unreliable. Experimental data are necessary.

Measurement of the thermal conductivities of hydride-forming materials under hydrogen pressure is difficult because the results can be significantly affected by hydriding or dehydriding reactions. Therefore, reactive materials must be contaminated with oxygen or other impurities (by deactivation) to prevent hydriding. There have been two previous conductivity measurements of this type of material. Yu, Suuberg, and Wade (*9*) reported the conductivity of deactivated iron–titanium hydride, and Reilly and Wiswall (*10*) reported conductivity for deactivated alloy. The former results were about 1.5 times the latter. Both of these earlier studies covered a range of hydrogen pressure similar to that used in our study, but temperature dependence was not measured. This paper examines both the pressure and the temperature dependence of effective thermal conductivity. Since heat from hydriding reactions appears to be the major source of error in previous studies, special care was taken to minimize reaction effects and to test for their presence. Also included are the conductivities with several cover gases, which can be used to evaluate the significance of the gas phase. The effective conductivity values reported include the heat transferred through the gas and the solid by conduction and by radiation, but the temperatures of these measurements were low enough that radiation is not expected to make a significant contribution. The overall values reported include all mechanisms and steps contributing to heat transfer through the powder.

Table I. Size Distribution of Deactivated Iron–Titanium Hydride Granules

size			fraction of total, wt %)
U.S. mesh		range, mm	
−8	+12	2.4–1.7	1.30
−12	+16	1.7–1.2	20.96
−16	+20	1.2–0.84	19.12
−20	+35	0.84–0.50	31.95
−35	+50	0.50–0.30	23.58
−50	+70	0.30–0.21	2.16
−70		<0.21	0.94
			100.01

Materials

Iron–titanium alloy was obtained from the MPD Technology Corp. (HY-STOR Alloy 101, Lot T-82878, Waldwich, NJ). It was exposed to air and used as received. Table I shows the particle size distribution of the alloy granules. The alloy has a density of 6.45 g/cm^3, and the bed was packed to a density of 3.65 g/cm^3.

The reticulated aluminum foam tested as a heat-transfer-promotion material was manufactured by Energy Research and Generation, Inc. (Oakland, CA). The foam was 91.8% voids (that is, 8.2 vol % aluminum) and contained interconnecting holes (open cells) with radii of approximately 0.05 in. (0.127 cm). The foam, which was machined to fit snugly into the test cell, was very porous and could be filled with Fe–Ti powder simply by pouring the powder into the foam.

Experimental Procedure

A transient technique was employed by using the test cylinder shown in Figure 1. The Fe–Ti or Al–Fe–Ti test samples were packed into a 1.375 in. (3.492 cm) i.d. stainless tube with 0.0675 in. (0.171 cm) thick walls. The 10-in. (25.4-cm) test section was insulated at both ends to minimize end effects. Temperature measurements were made at three different axial positions along the center line of the tube. The thermocouple locations were fixed and aligned by means of holes drilled

† Fractionation Research, Inc., South Pasadena, CA 91030.

0021-9568/85/1730-0369$01.50/0

Table II. Thermal Conductivities of the Deactivated Iron-Titanium Hydride Bed at the Pressure of Hydrogen

	K_h, Btu/(h·ft·°F) [W/(m·K)]				
temp, °C	1 atm	75 psig	200 psig	350 psig	500 psig
9	0.94 [1.63]	1.08 [1.87]	1.13 [1.96]	1.16 [2.01]	1.19 [2.06]
24	1.05 [1.82]	1.14 [1.97]	1.18 [2.04]	1.20 [2.08]	1.23 [2.13]
35	1.11 [1.92]	1.18 [2.04]	1.21 [2.09]	1.24 [2.15]	1.26 [2.18]
45	1.16 [2.01]	1.22 [2.11]	1.24 [2.15]	1.26 [2.18]	1.28 [2.22]
55	1.20 [2.08]	1.26 [2.18]	1.28 [2.22]	1.30 [2.25]	1.31 [2.27]
65	1.25 [2.16]	1.27 [2.20]	1.30 [2.25]	1.32 [2.28]	1.34 [2.32]
75	1.29 [2.23]	1.30 [2.25]	1.32 [2.29]	1.35 [2.34]	1.37 [2.37]

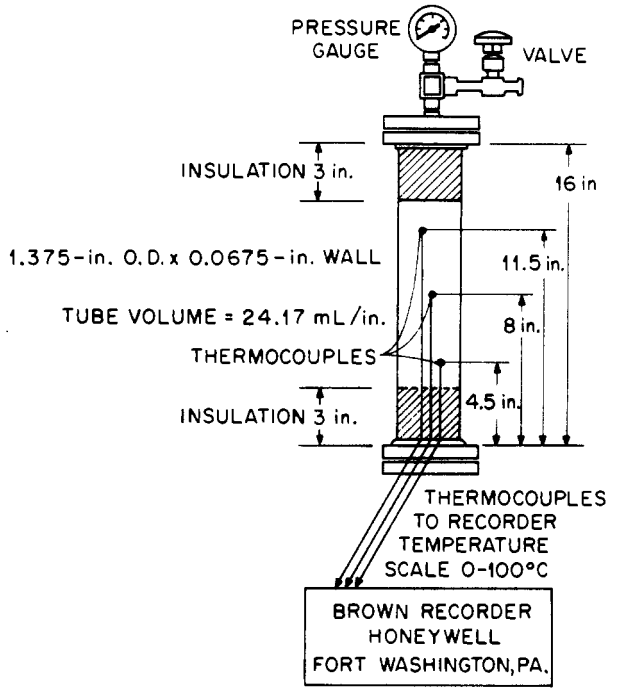

Figure 1. Experimental test cylinder.

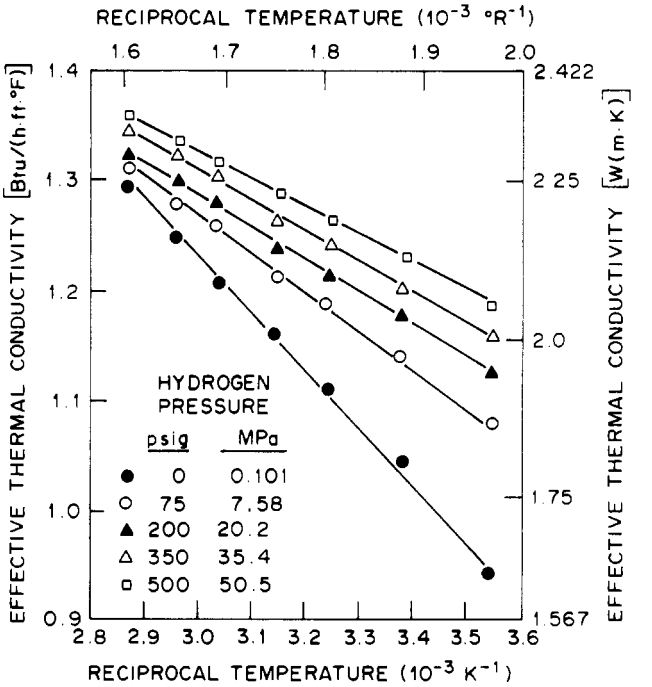

Figure 2. Temperature dependence of the thermal conductivity of deactivated iron–titanium hydride bed filled with hydrogen.

through the insulation at the lower end of the test section. Thus, no movement of the thermocouples was detected during the course of the experiment. The agreement between the temperature measurements at different axial positions demonstrated that the insulation reduced end effects to insignificant levels.

The test section was equilibrated at one temperature and then immersed into a circulating bath at either a higher or a lower temperature. The center-line temperature was then recorded as a function of time until it approached the bath temperature. Two baths were employed so that sequential runs could be made simply by transferring the test section from one bath to the other. The volumes of the temperature baths were sufficiently large that the immediate bath temperature change (momentarily) was less than 0.5 °C upon immersion of the test cell. The initial temperature differentials (differences between the temperature of the bath and that of the initial test section) were kept small, usually ±10 °C. This procedure permitted a good assessment of the variation of thermal conductivity with temperature. Results obtained with increasing and decreasing temperature were identical, indicating that chemical reaction did not occur during the measurements.

Thermal conductivity measurements were made both with and without Fe–Ti powder and with a variety of gases and pressures. Data were analyzed by using the classical equation for heat transfer in cylindrical geometry. The thermal conductivity of the Fe–Ti powder was so much lower than that of the thin stainless steel shell surrounding the powder that thermal resistance in the shell could be neglected. The equation for temperature at the center of a cylinder with an initial uniform temperature T_1 and with a surface temperature suddenly changed to T_0 is given in standard textbooks (*11*).

$$\frac{T - T_1}{T_0 - T_1} = 1 - 2\sum_{n=1}^{\infty} \frac{\exp(-\lambda \Psi_n^2 t)}{Zn J_1(Zn)}$$

where $Zn = a\Psi_n$ = roots of the Bessel function of zero order, a = radius of the cylinder, λ = thermal diffusivity of the powder, $J_1(Zn)$ = Bessel function of order 1, $K = \lambda C_p \rho$ = thermal conductivity of the powder, C_p = bulk heat capacity of the powder (from ref 2), and ρ = bulk density of the hydride powder (from ref 2). A least-squares routine was used to fit the experimental data to this equation and thus evaluate the best values for λ (and K). Details of the analyses are given in ref 12 and 13.

Results and Discussion

The thermal conductivities of iron–titanium hydride powders are shown in Table II and Figure 2 as a function of temperature and hydrogen pressure. Each measurement was made with a 10 °C (10 K) change in bed temperature, and the temperatures shown in Table II and Figure 2 are the midpoints of those ranges. The center-line temperature-vs.-time curves were fitted (using a least-squares method) to the curves predicted for a constant thermal conductivity over this temperature range. Similar data were taken with the Fe–Ti powder under helium pressure for comparison. Since helium does not react with the Fe–Ti, similarities between the conductivity data with helium and hydrogen provide further evidence that the hydrogen data were not affected by hydriding/dehydriding reactions (i.e., no reactions

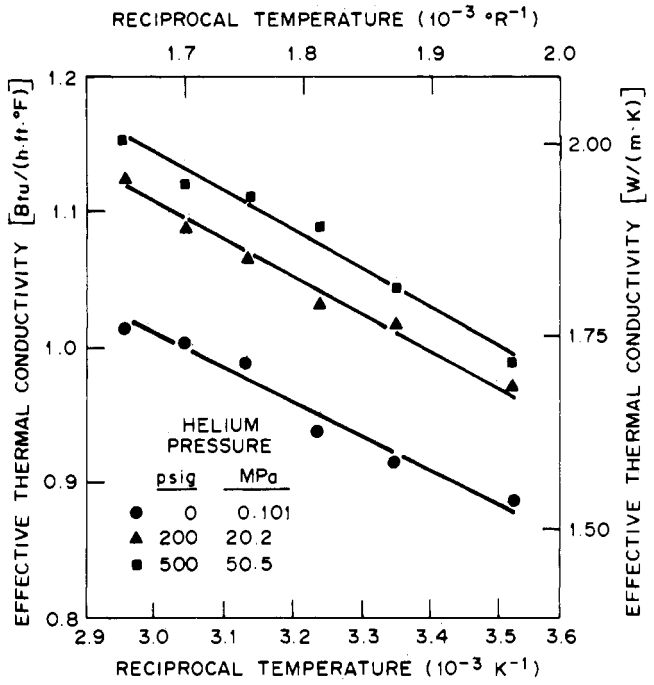

Figure 3. Temperature dependence of the thermal conductivity of deactivated iron–titanium hydride bed filled with helium.

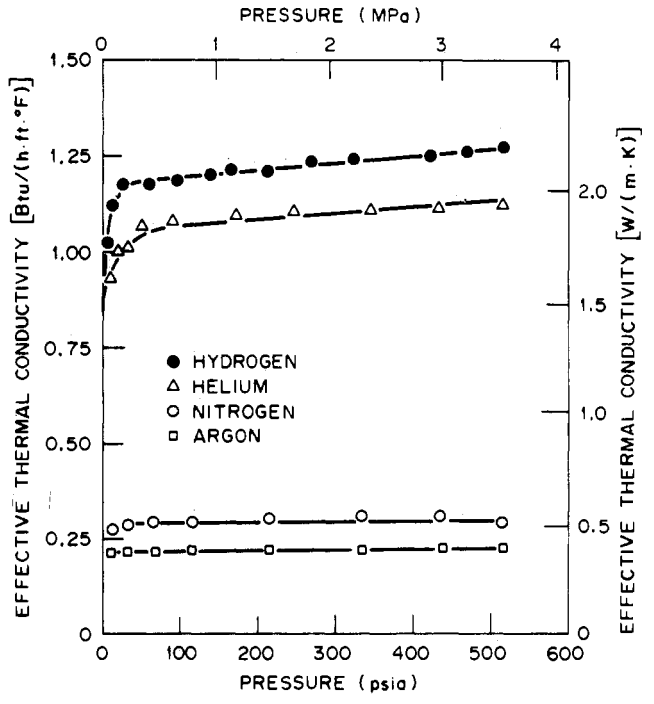

Figure 4. Pressure dependence of the thermal conductivity of deactivated iron–titanium hydride filled with hydrogen, helium, nitrogen, and argon at 30–50 °C.

occurred). The plot of the helium results, shown in Figure 3, is indeed similar in shape to that for hydrogen in Figure 2. The thermal conductivities with helium are less than those with hydrogen, as expected, since the thermal conductivity of helium gas is less than that of hydrogen.

The effects of gas pressure on the thermal conductivity of the Fe–Ti powder are shown in Figure 4. These measurements were taken over the temperature range of 30–50 °C (a 20 °C change in the test section temperature during the measurement) with helium, nitrogen, and argon fill gas, as well as hydrogen. Note that the thermal conductivity of the bed varies, as expected, with the gas used: $K_{H_2} > K_{He} > K_{N_2} > K_{Ar}$. There are no indications that hydriding reactions have affected

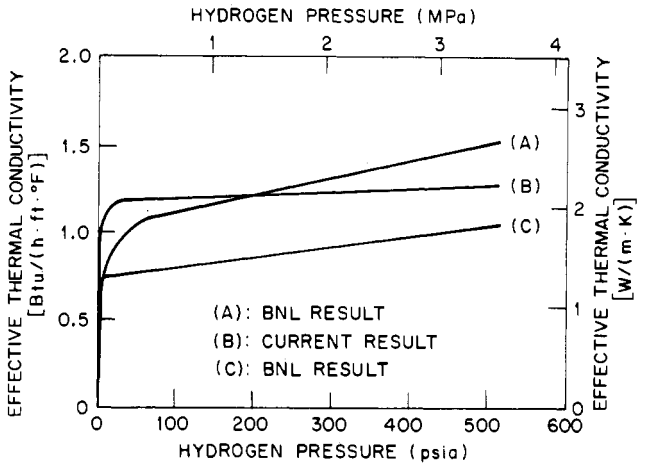

Figure 5. Comparison of current measurements of the conductivity of deactivated iron–titanium hydride in hydrogen (curve B) with previous measurements from ref 9 (curve A) and from ref 10 (curve C).

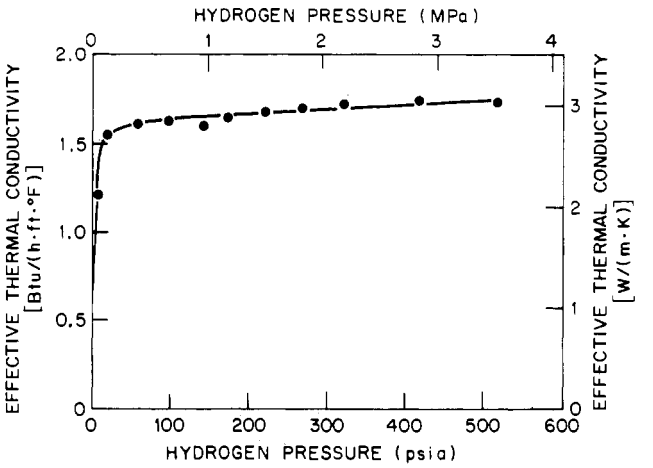

Figure 6. Thermal conductivity of deactivated iron–titanium hydride in aluminum foam (r_m = 0.05 in., Va = 8.2%) as a function of hydrogen pressure (measured at 30–50 °C).

the hydrogen curve. There is an initial rapid increase in thermal conductivity with gas pressure followed by a much slower increase; however, the curves for the four gases are similar.

The hydrogen curve shown in Figure 4 has been compared with previous data reported from two earlier studies (*9*, *10*) (see Figure 5). The present data generally lie between the earlier curves, except at low pressures where they are slightly above both previous sets of data. The present data are accompanied with much stronger indications that there were no hydriding/dehydriding reactions, no end effects, and better fits to the expected temperature-vs.-time curves. Thus, these new data are believed to be more accurate and more reliable.

The thermal conductivity of the aluminum foam filled with Fe–Ti is shown in Figure 6 as a function of hydrogen pressure. Note that the thermal conductivity is increased by adding the aluminum foam (the curve in Figure 6 is approximately 1.4 times that for hydrogen in Figure 4).

Conclusions

New measurements of thermal conductivity of beds containing deactivated Fe–Ti granules covering a range of hydrogen overpressures show no indications that significant hydriding or dehydriding reactions occurred. The results are believed to be the most reliable for evaluating the performance of this highly fractured material in a number of proposed hydriding (hydrogen storage) applications. These data differ significantly from some previous measurements. The use of an aluminum foam structure to increase the thermal conductivity of the bed did

have a small, but potentially significant, positive effect.

Registry No. HY-STOR Alloy 101, 77980-77-9; hydrogen, 1333-74-0; aluminum, 7429-90-5.

Literature Cited

(1) Reilly, J. J.; Sandrock, G. D. *Sci. Am.* **1980**, *242*, 118-29.
(2) Reilly, J. J.; Wiswall, R. H., Jr. *Inorg. Chem.* **1974**, *13*, 218.
(3) Lundin, C. E.; Liu, J.; Megee, C. B. "Development of Hydrogen Storage Material for Application to Energy Needs"; Proceedings Chemical/Hydrogen Energy Systems Contracts Review, Washington, DC, Nov 27-30, 1978.
(4) Clinch, J. M.; Gruen, D. M.; Nelson, P. A.; Blomquist, C. A.; Horowitz, J. S.; Lamich, G. J.; Sheft, I. "The Metal Hydride Chemical Heat Pump"; Proceedings Chemical/Hydrogen Energy Systems Contracts Review, Washington, DC, Nov 13-14, 1979.
(5) Fisher, P. W.; Watson, J. S. "Modeling Solid Hydrogen Storage Beds"; Proceedings Chemical/Hydrogen Energy Systems Contracts Review, Washington, DC, Nov 13-14, 1979.
(6) Fisher, P. W.; Watson, J. S. In "Hydrogen Energy Progress"; Veziroglu, T. N., et al., Eds.; Pergamon Press: Elmsford, NY, 1980; pp 839-47.
(7) Strickland, G.; Yu, W. S. "Some Rate and Modeling Studies on the Use of Iron-Titanium Hydride as an Energy Medium for Electrical Utility Companies", BNL-50667; Brookhaven National Laboratory: Upton, NY, April 26, 1977.
(8) Rosso, M. J., Jr.; Strickland, G. "Hydride Beds: Engineering Tests"; Proceedings Chemical/Hydrogen Energy Systems Contracts Review, Washington, DC, Nov 13-14, 1979.
(9) Yu, W. S.; Suuberg, E.; Wade, C. In "Hydrogen Energy Part A"; Veziroglu, T. N., Ed.; Plenum Press: New York, 1975; pp 621-43.
(10) Reilly, J. J.; Wiswall, R. H., Jr. "Hydrogen Storage and Purification System", BNL-19436; Brookhaven National Laboratory: Upton, N.Y, Aug 1, 1974.
(11) Carslaw, H. S.; Jaeger, J. C. "Conduction of Heat in Solids", 2nd ed.; Oxford Press: London, 1959; p 199.
(12) Lin, T. H. Ph.D. Dissertation, University of Tennessee, Knoxville, TN, 1981.
(13) Lin, T. H.; Watson, J. S. "Heat Transfer in Iron-Titanium Hydride Beds", ORNL/TM-8982, in press.

Received for review March 21, 1984. Revised manuscript received October 29, 1984. Accepted November 19, 1984. This research was sponsored by the Office of Basic Energy Sciences, U.S. Department of Energy, under Contract DE-AC05-84OR21400 with Martin Marietta Energy Systems, Inc.

Vaporization Study of *o*-, *m*-, and *p*-Chloroaniline by Torsion-Weighing Effusion Vapor Pressure Measurements

V. Piacente,* P. Scardala, D. Ferro, and R. Gigli

Dipartimento di Chimica, Università "La Sapienza", Roma, Italy

A combined torsion-weighing effusion apparatus was used to measure the vapor pressures of *o*-, *m*-, and *p*-chloroaniline; their temperature dependences are given by the equations: *o*-chloroaniline, log *P* (kPa) = (8.63 ± 0.16) − (3006 ± 56)/*T*; *m*-chloroaniline, log *P* (kPa) = (8.86 ± 0.10) − (3180 ± 40)/*T*; *p*-chloroaniline, log *P* (kPa) = (11.20 ± 0.20) − (4170 ± 60)/*T*. The standard vaporization enthalpies $\Delta H°_{298}$ = 57.5 ± 5, 60.9 ± 5, and 79.0 ± 5 kJ mol^{-1} for *o*-, *m*-, and *p*-chloroaniline, respectively, were derived. Free energy functions of the gaseous and solid phase for these compounds are also reported.

Introduction

Except for the old values selected by Ohe (*1*) and those referred to *o*- and *m*-chloroaniline published by Walton (*2*), not accessible to us, apparently no other vapor pressure data for *o*-, *m*-, and *p*-chloroaniline are reported in literature.

In view of filling this lack of experimental data and as a part of our continuing research program on the determination of the thermodynamic properties associated with the vaporization of organic compounds, the vapor pressure of *o*-, *m*-, and *p*-chloroaniline were measured by using a combined torsion-weighing effusion apparatus.

Experimental Apparatus

The assembly used to measure the vapor pressure of *o*-, *m*-, and *p*-chloroaniline consists of a conventional torsion–effusion apparatus suspended from one arm of an automatic vacuum electrobalance. Figure 1 shows a schematic representation of the apparatus. The graphite effusion cell was of standard design. Moment arms and thickness of the effusion holes were measured by photographic enlargement. Effective orifice area was obtained by appropriate use of Freeman's (*3*) and Clausing's (*4*) equations in the torsion and Knudsen measurements, respectively. Temperature of the cell, heated by a fluidized sand bath Tecam SLB-1 thermostated within ±0.1 °C, was measured by a calibrated iron–copper thermocouple inserted in a second graphite cell placed at the same level of the effusion one and continuosly recorded by a Philips PM 8252 potentiometer. However, the overall accuracy of the reported temperature must be estimated at ±2 °C considering the uncertainty in the measurement (±1 × 10^{-3} mV) and in the junction potentials. Background pressure of the system during the vaporizations was always less than 2 × 10^{-5} torr.

The vapor pressures were measured by simultaneous Knudsen and torsion–effusion methods. The pressure values determined from thermogravimetric data were obtained by the following form of the Knudsen equation (*5*)

$$P\,(\text{kPa}) = \frac{38.2}{A_1 + A_2}\,(T/M)^{1/2}\,dg/dt$$

where A_1 and A_2 are the effective areas of the effusion orifices in cm^2, M the molecular weight of the vapor, T the cell temperature in Kelvin, and dg/dt the weight loss rate of the sample in milligrams/minute. The weight loss rate was determined under steady-state conditions by a Cahn RH vacuum microbalance coupled with an automatic recording of the mass loss of the sample as a function of time and a time derivative computing. The error in the rate measurement, which is a function of chart speed and balance sensitivity, is less than 1%. The errors due to variations in chart shrinkage or speed and in balance sensitivity were found to be negligible.

Simultaneously, at each experimental temperature, the vapor pressure was determined by the well-known torsion–effusion equation (*6*)

$$P = \frac{2\alpha K}{A_1 {}^{\circ}l_1 + A_2 {}^{\circ}l_2}$$

where K is the torsion constant of the torsion tungsten wire,

0021-9568/85/1730-0372$01.50/0